Error Propagation and Formation Structure Design using Dual Quaternion Algebra

Xiangke Wang, Changbin Yu and Zhiyun Lin

Abstract— **By utilizing a new mathematical tool, i.e., unit dual quaternion and its logarithmic norm, the problem of error propagation and its upper bound on rotation and translation in one path of a rooted tree in 3-dimensional space is studied. For prescribed angular and distance error thresholds, a maximum depth of the rooted tree is obtained correspondingly, which can be used to guide the structure design for formations. Finally, the maximum depth condition is validated by simulations on the USARSim platform with quad-rotor formations.**

I. INTRODUCTION

Error propagation has been studied in many domains, such as wireless sensor network (WSN) localization [1], simultaneous localization and mapping (SLAM) [2], and multi-body system [3], but seldom studied in multiple rigid-body formation where errors are inevitable in practical applications. Moreover, almost all existing work is only confined to 3 rotational DOF (degree-of-freedom) or 3 translational DOF, and cannot be directly extended to 3-D (3-dimensional) space with 6 DOF because of the interconnection between rotation and translation. Here, 6 DOF includes 3 rotational DOF and 3 translational DOF. And we use *rigid-body* to express the fully actuated robots/spacecrafts in 3-D space. In this study, we pay attention to the error propagation problem between rigid-bodies. Especially, the transmission and accumulation of the steady-state errors, which may come from the sensing, control and/or actuation, along a path in 3-D space, irrespective of the control law or measuring technique. The string stability and the mesh stability of the interconnected systems, which are proposed and studied in [4] and [5] to indicate a kind of transient properties of the entire formation, are somehow related to the error propagation problem studied in this paper.

(Directed and undirected) graphs are used widely to describe the interconnection of formations, and different graph based results have been conducted, see e.g. [6]–[10]. Among these different results, we note that in [8], it is proved that formation stabilization is feasible if and only if the sensor graph has a globally reachable node. A rooted tree is the most fundamental and simplest digraph including a globally reachable node, while different rooted trees can be constructed for a multiple rigid-body system. When considering the error propagations along the paths and a given safety bound on the formation error, only parts of the rooted trees can satisfy the safety bound. How to find the conditions, especially the depth constraint of the rooted tree, and use them to guide the formation structure design such that the given bound can be satisfied, is another issue in this study.

Our analysis is carried out using unit dual quaternion representations of rigid-bodies. Section II will offer further details about unit dual quaternion representations, but here we provide some discussions on relevant literature. The unit dual quaternion is a natural extension of the unit quaternion, and essentially it belongs to a Plücker coordination in 6 DOF. It is well known that the unit quaternion provides an efficient global representation for rotation without singularity; and similarly the unit dual quaternion is an efficient tool to represent a transformation (including rotation and translation simultaneously) globally without singularity with only 8 numbers. As stated by some literature, for examples, [11]–[13], the unit dual quaternion is the most compact and efficient way to express the transformation. In [14] and [15], the logarithmic feedback of unit dual quaternion is utilized to derive controllers, which can control rotation and translation simultaneously. In many applications, such as image-based localization [16], eye-hand calibration [17], navigation [18], and manipulator control [19], unit dual quaternions are all elegant and useful tool.

We formulated the studied problems with dual quaternion descriptors in Section III. And in Section IV, the error propagation between multiple rigid-bodies along one path is expressed by unit dual quaternion algebra. Then by utilizing some properties of the logarithmic norm of unit dual quaternions, Section V provides an upper bound of the error propagation on rotation and translation. Considering both angular and distance error thresholds, a maximum number of rigid-bodies allowed to be embodied in one path, or the maximum depth of the rooted tree, is obtained correspondingly, which can be used to guide the structure design for formations. The proposed depth conditions are validated on the urban search and rescue simulation (USARSim) platform with quad-rotors in Section VI. Finally, the last section draws the conclusions.

II. MATHEMATIC PRELIMINARIES

In this section, for the convenience of the reader, we restate some basic notions about the dual quaternion.

X. Wang is with College of Mechatronics and Automation, National University of Defense Technology, 410073, China, supported in part by the China Scholarship Council and NICTA Ltd. xkwang@nudt.edu.cn
C. Yu is with the Australian National University and NICTA Ltd, Canberra, A.C.T., Australia, and also with Shandong Computer Science Center, Jinan, China. The work of C. Yu is supported by the Australian Research Council through a Queen Elizabeth II Fellowship and DP-110100538 and Overseas Expert Program of Shandong Province. brad.yu@anu.edu.au
Z. Lin is with College of Electrical Engineering, Zhejiang University, Hangzhou, China, supported by National Natural Science Foundation of China (60875074). linz@zju.edu.cn

A *quaternion* is an extension of a complex number to $\mathbb{R}^4$. Formally, a quaternion is defined as

$$q = [s, \boldsymbol{v}], \tag{1}$$

where s is a scalar (called the *scalar part*), and $\boldsymbol{v}$ is a three-dimensional vector (called the *vector part*). The conjugate of a quaternion q given in (1) is $q^* = [s, -\boldsymbol{v}]$. For two quaternions $q_1 = [s_1, \boldsymbol{v}_1]$ and $q_2 = [s_2, \boldsymbol{v}_2]$, the *addition* and the *multiplication* operations are, respectively, defined

$$q_1 + q_2 = [s_1 + s_2, \boldsymbol{v}_1 + \boldsymbol{v}_2], \tag{2}$$

$$q_1 \circ q_2 = [s_1 s_2 - \boldsymbol{v}_1^T \boldsymbol{v}_2, s_1 \boldsymbol{v}_2 + s_2 \boldsymbol{v}_1 + \boldsymbol{v}_1 \times \boldsymbol{v}_2]. \tag{3}$$

If $q \circ q^* = Q_I = [1, 0, 0, 0]$, then q is called a *unit quaternion*.

A *dual number* is defined as

$$\hat{a} = a + \epsilon b \quad \text{with} \quad \epsilon^2 = 0, \quad \text{but} \quad \epsilon \neq 0, \tag{4}$$

where a and b are real numbers, called the *real part* and the *dual part*, respectively, and ϵ is nilpotent. To compare two dual numbers, the *partial order* is defined as follows.

Definition 1 (Partial Order): Given two dual numbers $\hat{v}_1 = v_{r1} + \epsilon v_{d1}$ and $\hat{v}_2 = v_{r2} + \epsilon v_{d2}$, if $v_{r1} - v_{r2} \geq (>) 0$ and $v_{d1} - v_{d2} \geq (>) 0$, then we say $\hat{v}_1 \geq (>) \hat{v}_2$.

Dual vectors are a generalization of dual numbers whose real and dual parts are both three-dimensional vectors.

A *dual quaternion* is a quaternion with dual number components, i.e.,

$$\hat{q} = [\hat{s}, \hat{\boldsymbol{v}}], \tag{5}$$

where $\hat{s}$ is a dual number and $\hat{v}$ is a dual vector. Clearly, a three-dimensional (dual) vector can also be treated equivalently as a (dual) quaternion with a vanishing real part, called *(dual) vector quaternion*. If not otherwise stated, a (dual) vector is denoted by the boldface, and its corresponding (dual) vector quaternion is denoted by the normal type, for example, $v = [0, \boldsymbol{v}]$ or $\hat{v} = [0, \hat{\boldsymbol{v}}]$.

The dual quaternion also can be treated as a dual number with quaternion components, which is

$$\hat{q} = q_r + \epsilon q_d, \tag{6}$$

where q_r and q_d are both quaternions.

The *conjugate* of a dual quaternion $\hat{q}$ given by (5) or (6) is

$$\hat{q}^* = [\hat{s}, -\hat{\boldsymbol{v}}] = q_r^* + \epsilon q_d^*. \tag{7}$$

For two dual quaternions $\hat{q}_1 = q_{r1} + \epsilon q_{d1}$ and $\hat{q}_2 = q_{r2} + \epsilon q_{d2}$, the *addition* and the *multiplication* are

$$\hat{q}_1 + \hat{q}_2 = (q_{r1} + q_{r2}) + \epsilon(q_{d1} + q_{d2}), \tag{8}$$

$$\hat{q}_1 \circ \hat{q}_2 = q_{r1} \circ q_{r2} + \epsilon(q_{r1} \circ q_{d2} + q_{d1} \circ q_{r2}), \tag{9}$$

respectively. If $\hat{q} \circ \hat{q}^* = \hat{Q}_I = [1, 0, 0, 0] + \epsilon[0, 0, 0, 0]$, then the dual quaternion $\hat{q}$ is called a *unit dual quaternion*.

Unit quaternions can be used to describe rotations. For the frame rotation about the unit axis $\boldsymbol{n}$ with an angle $|\theta| < 2\pi$, there is a unit quaternion

$$q = [\cos(\frac{|\theta|}{2}), \sin(\frac{|\theta|}{2})\boldsymbol{n}], \tag{10}$$

relating a fixed vector expressed in the original frame $\boldsymbol{r}^o$ with the same vector expressed in the new frame $\boldsymbol{r}^n$ by

$$r^n = q^* \circ r^o \circ q. \tag{11}$$

Note that r^o and r^n in (11) are two vector quaternions.

A unit dual quaternion can be used to represent a transformation (rotation and translation simultaneously) in 3-D space. Considering a rotation q succeeded by a translation $\boldsymbol{p}^b$, according to the Chasles Theorem (refer to Theorem 2.11, [20]), this transformation is equivalent to a screw motion, which is a rotation about an axis $\boldsymbol{n}$ with angel $|\theta|$ combined with a translation d parallel to $\boldsymbol{n}$ illustrated in Fig. 1. The transformation can be represented using a unit dual quaternion [1]

$$\hat{q} = [\cos\frac{\hat{\theta}}{2}, \sin\frac{\hat{\theta}}{2}\hat{\boldsymbol{n}}] = q + \frac{\epsilon}{2} q \circ p^b, \tag{12}$$

where $\hat{\boldsymbol{n}} = \boldsymbol{n} + \epsilon(\boldsymbol{c} \times \boldsymbol{n})$ is the screw axis, in which $\boldsymbol{c}$ is the vector from the original position to the rotational center (see in Fig. 1), and $\hat{\theta} = |\theta| + \epsilon d$ is the dual angle of the screw [18].

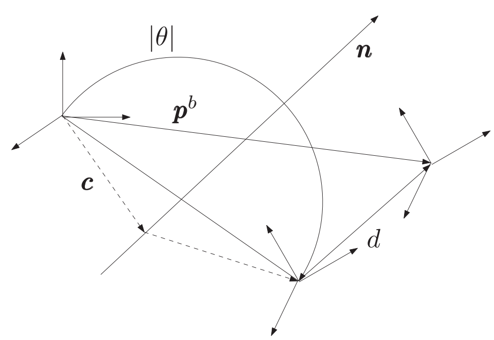

Fig. 1. Geometry of screw motion

A unit quaternion q serves as a rotation, taking coordinates of a point from one frame to another. On the other hand, every orientation of a rigid-body that is free to rotate relative to a fixed frame can be identified with a unique unit quaternion q. Analogous to the rotational case, a unit dual quaternion $\hat{q}$ serves as both a specification of the configuration (consisting of orientation and position) of a rigid-body and a transformation taking the coordinates of a point from one frame to another.

The logarithm of a unit quaternion defined in (10) is defined as [21]

$$\ln q = \frac{|\theta|}{2}\boldsymbol{n}. \tag{13}$$

Similarly, the logarithmic mapping of a unit dual quaternion given by (12) is defined as [14]

$$\ln \hat{q} = \frac{1}{2}(\theta + \epsilon p^b), \tag{14}$$

[1] Superscripts b and s relate to the body-frame (which is attached to the body) and the spatial-frame (which is relative to a fixed (inertial) coordinate frame) respectively throughout this paper. The concepts of body-frame and spatial-frame come from [20].

where $\theta = [0, \boldsymbol{\theta}]$ with $\boldsymbol{\theta} = |\theta|\boldsymbol{n}$ and $p^b = [0, \boldsymbol{p}^b]$.

Given a (dual) vector quaternion v ($\hat{v}$) and a unit (dual) quaternion q ($\hat{q}$), the *adjoint transformation* is defined as

$$Ad_q v = q \circ v \circ q^* \quad \text{or} \quad Ad_{\hat{q}} \hat{v} = \hat{q} \circ \hat{v} \circ \hat{q}^*. \tag{15}$$

The *left-invariant error* from a unit dual quaternion $\hat{q}$ to $\hat{q}_d$ is defined as

$$\hat{q}_e = \hat{q}_d^* \circ \hat{q} = q_e + \frac{\epsilon}{2} q_e \circ p_e^b, \tag{16}$$

where $q_e = q_d^* \circ q$ and $p_e^b = p^b - Ad_{q_e^*} p_d^b$. The left-invariant error describes the relative configuration or the mismatch between two configurations in terms of unit dual quaternions. It should be noted that if $\hat{q}_e = \pm \hat{Q}_I$, then $\hat{q} = \hat{q}_d$.

III. PROBLEM FORMULATION

Consider a group of $n+1$ rigid-bodies in 3-D space with their configurations expressed by unit dual quaternions, i.e.,

$$\hat{q}_i = q_i + \frac{\epsilon}{2} q_i \circ p_i^b, \quad i = 0, \ldots, n. \tag{17}$$

We call the group of rigid-bodies expressed by (17) the *overall system* throughout this paper.

In this study, we consider a *rooted tree* to represent the interconnections of the overall system, whose nodes are $N = \{0, 1, \ldots, n\}$ representing rigid-bodies, and arcs $V = \{(i,j), i,j \in N\}$ describing the control/sensing interconnections between rigid-bodies, with all necessary relative orientations and positions available. In the rooted tree, there is only one *lead* – the one without neighbors, and except for the lead, each rigid-body has only one *neighbor*. The nodes who are not neighbors of any other nodes are called *leaf nodes*.

The objective of this paper is to study the error propagation problem, viz. the accumulation of errors along one path, in the rooted tree by using unit dual quaternion algebra, and then to find some conditions to guide the structure design for the overall system, such that the given safety bound on the formation error can be satisfied.

IV. ERROR PROPAGATION

In this section, we represent the error propagation along one path by unit dual quaternion algebra.

We can construct a path in the rooted tree. Denote the rigid-bodies in the path from the lead to the leaf node by rigid-body $0, \ldots, i, i+1, \ldots, k$ ($i < k$), where rigid-body i is the neighbor of rigid-body $i+1$, namely rigid-body $i+1$ can obtain its relative configuration to rigid-body i. For $i = 0, \ldots, k-1$, denote the specified and the actual relative configurations from rigid-body $i+1$ to rigid-body i by

$$\hat{q}_{d_{i(i+1)}} = q_{d_{i(i+1)}} + \frac{\epsilon}{2} q_{d_{i(i+1)}} \circ p_{d_{i(i+1)}}^b, \tag{18}$$

$$\hat{q}_{i(i+1)} = q_{i(i+1)} + \frac{\epsilon}{2} q_{i(i+1)} \circ p_{i(i+1)}^b, \tag{19}$$

respectively, shown in Fig. 2. Here the specified relative configuration is the desired one without any errors. However, because of errors, the actual relative configuration cannot coincide to the specified relative configuration. According to (16), the mismatch (left-invariant error) $\hat{q}_{e_{(i+1)'(i+1)}}$ from $\hat{q}_{i(i+1)}$ to $\hat{q}_{d_{i(i+1)}}$ is

$$\begin{aligned}\hat{q}_{e_{(i+1)'(i+1)}} &= \hat{q}_{d_{i(i+1)}}^* \circ \hat{q}_{i(i+1)} \\ &= q_{e_{(i+1)'(i+1)}} + \frac{\epsilon}{2} q_{e_{(i+1)'(i+1)}} \circ p_{e_{(i+1)'(i+1)}}^b,\end{aligned} \tag{20}$$

where $q_{e_{(i+1)'(i+1)}} = q_{d_{i(i+1)}}^* \circ q_{i(i+1)}$ and $p_{e_{(i+1)'(i+1)}}^b = p_{i(i+1)}^b - Ad_{q_{e_{(i+1)'(i+1)}}^*} p_{d_{i(i+1)}}^b$.

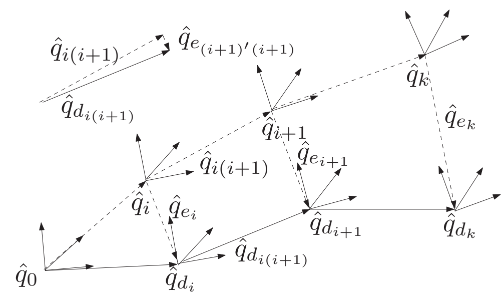

Fig. 2. Illustration of the rigid-bodies in on path.

Before obtaining the error propagation representation of $n+1$ linked rigid-bodies in one path, we present a preliminary result first regarding the relationship between two rigid-bodies.

Property 1: If the configurations of rigid-bodies i and j are $\hat{q}_i$ and $\hat{q}_j$ with respective to a inertial frame, and the transformation (relative configuration) from rigid-body i to j is $\hat{q}_{ij}$, then $\hat{q}_j = \hat{q}_i \circ \hat{q}_{ij}$.

An illustration of the property is shown in Fig. 3.

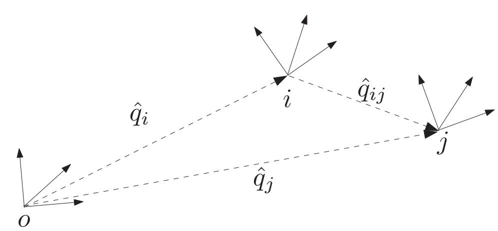

Fig. 3. Transformation in terms of unit dual quaternions.

Using Property 1, the specified and actual configurations of rigid-body k should be

$$\hat{q}_{d_k} = \hat{q}_0 \circ \hat{q}_{d_{01}} \circ \ldots \circ \hat{q}_{d_{(k-2)(k-1)}} \circ \hat{q}_{d_{(k-1)k}}, \tag{21}$$

$$\hat{q}_k = \hat{q}_0 \circ \hat{q}_{01} \circ \ldots \circ \hat{q}_{(k-2)(k-1)} \circ \hat{q}_{(k-1)k}. \tag{22}$$

After some operations, the left-invariant error $\hat{q}_{e_k}$ is

$$\begin{aligned}\hat{q}_{e_k} =& \hat{q}_{d_k}^* \circ \hat{q}_k \\ =& Ad_{\hat{q}_{d_{(k-1)k}}^*} \big(Ad_{\hat{q}_{d_{(k-2)(k-1)}}^*} \cdots \\ & (Ad_{\hat{q}_{d_{12}}^*} \hat{q}_{e_{1'1}} \circ \hat{q}_{e_{2'2}}) \ldots \circ \hat{q}_{e_{(k-1)'(k-1)}} \big) \circ \hat{q}_{e_{k'k}}.\end{aligned} \tag{23}$$

Clearly, $\hat{q}_{e_k}$ in (23) can be represented with an iterative form as follows:

$$\hat{q}_{e_1} = \hat{q}_{e_{1'1}}, \tag{24}$$

$$\hat{q}_{e_{i+1}} = Ad_{\hat{q}_{d_{i(i+1)}}^*} \hat{q}_{e_i} \circ \hat{q}_{e_{(i+1)'(i+1)}}, i = 1, \ldots, k-1. \tag{25}$$

In (24) and (25), the term $Ad_{\hat{q}^*_{d_{i(i+1)}}}\hat{q}_{e_i}$ could be understood as the propagation of errors from rigid-body i to rigid-body $i+1$, while $\hat{q}_{e_{(i+1)'(i+1)}}$ could be understood as the errors accruing in rigid-body $i+1$. Thus, $\hat{q}_{e_k}$ in (25) represents error accumulations from rigid-body 0 to rigid-body k in one path.

Some special cases of $\hat{q}_{e_k}$ are given as follows.

When $k=1$ in (23)) or (24), we have

$$\hat{q}_{e_1} = \hat{e}_{1'1}. \tag{26}$$

When $k=2$ in (23) or (25), we have

$$\hat{q}_{e_2} = Ad_{\hat{q}^*_{d_{12}}}\hat{q}_{e_{1'1}} \circ \hat{q}_{e_{2'2}}. \tag{27}$$

When $k=3$ in (23) or (25), we have

$$\begin{aligned}\hat{q}_3 &= Ad_{\hat{q}^*_{d_{23}}}\hat{q}_{e_2} \circ \hat{q}_{e_{3'3}} \\ &= Ad_{\hat{q}^*_{d_{23}}}(Ad_{\hat{q}^*_{d_{12}}}\hat{q}_{e_{1'1}} \circ \hat{q}_{e_{2'2}}) \circ \hat{q}_{e_{3'3}}.\end{aligned} \tag{28}$$

V. UPPER BOUND AND FORMATION DESIGN

A. Upper bound on rotation and translation

To find some conditions to guide the structure design for the overall system, we often require the errors' upper bounds for each node k. To measure the errors in (24)–(25) and to deduce its upper bound on rotation and translation, we introduce the *Logarithmic Norm* of a unit dual quaternion.

Definition 2 (Logarithmic Norm): For a unit dual quaternion $\hat{q}$ given by (12), its *logarithmic norm* is defined as

$$|\ln\hat{q}| = |\boldsymbol{\theta}| + \epsilon|\boldsymbol{p}^b|, \tag{29}$$

where $|\boldsymbol{\theta}|$ and $|\boldsymbol{p}^b|$ are the amplitudes of $\boldsymbol{\theta}$ and $\boldsymbol{p}^b$, respectively.

Denote $\ln\hat{q}_{e_{i'i}} = \frac{1}{2}(\theta_{e_{i'i}} + \epsilon p^b_{e_{i'i}})$ for $i=1,\dots,k$. Clearly, $|\ln\hat{q}_{e_k}| = |\boldsymbol{\theta}_{e_k}| + \epsilon|\boldsymbol{p}^b_{e_k}|$ describes the error amplitudes on rotation and translation, where $|\boldsymbol{\theta}_{e_k}|$ is the angular error and $|\boldsymbol{p}^b_{e_k}|$ is the distance error.

For the logarithmic norm of unit dual quaternions, the following properties are hold, which can be verified by direct computations.

Property 2: Given a unit dual quaternion $\hat{q}$ defined in (12), we have $|\ln\hat{q}| = |\ln\hat{q}^*|$.

Property 3: For two unit dual quaternions $\hat{q}_1$ and $\hat{q}_2$ given by (12), the following inequality holds:

$$|\ln(\hat{q}_1 \circ \hat{q}_2)| \le |\ln\hat{q}_1| + |\ln\hat{q}_2|.$$

Property 4: Given two unit dual quaternions $\hat{q}_1$ and $\hat{q}_2$ defined by (12), and let $\ln\hat{q}_1 = \frac{1}{2}(\theta_1 + \epsilon p^b_1)$ and $\ln\hat{q}_2 = \frac{1}{2}(\theta_2 + \epsilon p^b_2)$, we obtain $|\ln(Ad_{\hat{q}^*_1}\hat{q}_2)| \le |\ln\hat{q}_2| + 2\epsilon|\boldsymbol{p}^b_1|\sin\frac{|\boldsymbol{\theta}_2|}{2}$.

Property 5: Let $\hat{q}_i$ $(i=1,2,3)$ be unit dual quaternions with $\ln\hat{q}_i = \frac{1}{2}(\theta_i + \epsilon p^b_i)$. Then

$$|\ln(Ad_{\hat{q}^*_1}\hat{q}_2 \circ \hat{q}_3)| \le |\ln\hat{q}_2| + |\ln\hat{q}_3| + 2\epsilon|\boldsymbol{p}^b_1|\sin\frac{|\boldsymbol{\theta}_2|}{2}.$$

Applying Property 5, the following result follows from the iterative form of $\hat{q}_{e_k}$ in (25) immediately.

Lemma 1: For $i=1,\dots,k-1$, from (24) and (25), it holds that

$$|\ln\hat{q}_{e_{i+1}}| \le |\ln\hat{q}_{e_i}| + |\ln\hat{q}_{e_{(i+1)'(i+1)}}| + 2\epsilon|\boldsymbol{p}^b_{d_{i(i+1)}}|\sin\frac{|\boldsymbol{\theta}_{e_i}|}{2},$$

where $\ln\hat{q}_{d_{i(i+1)}} = \frac{1}{2}(\theta_{d_{i(i+1)}} + \epsilon p^b_{d_{i(i+1)}})$, $\theta_{e_i} = 2\ln q_{e_i}$, and $|\ln\hat{q}_{e_1}| = |\ln\hat{q}_{e_{1'1}}|$.

Now we are ready to contribute our main result in Theorem 1. It is noted that the real and dual parts of the right-handed side of (30) in Theorem 1 reflect the upper bounds of $\hat{q}_{e_k}$ on angular error and distance error, respectively.

Theorem 1: For $i=1,\dots,k-1$, denote $\ln\hat{q}_{d_{i(i+1)}} = \frac{1}{2}(\theta_{d_{i(i+1)}} + \epsilon p^b_{d_{i(i+1)}})$ and $\ln\hat{q}_{e_{i'i}} = \frac{1}{2}(\theta_{e_{i'i}} + \epsilon p^b_{e_{i'i}})$. From (24) and (25), it holds that

$$|\ln\hat{q}_{e_k}| \le \sum_{i=1}^{k}|\boldsymbol{\theta}_{e_{i'i}}| + \epsilon(\sum_{i=1}^{k}|\boldsymbol{p}^b_{e_{i'i}}| + 2\sum_{j=1}^{k-1}|\boldsymbol{p}^b_{d_{j(j+1)}}|\sin\frac{|\boldsymbol{\theta}_{e_j}|}{2}). \tag{30}$$

Proof: We use induction to prove the theorem.

1) when $k=1$, from (26), we obtain

$$|\ln\hat{q}_{e_1}| = |\ln\hat{q}_{e_{1'1}}| = |\boldsymbol{\theta}_{e_{1'1}}| + \epsilon|\boldsymbol{p}^b_{e_{i'i}}|.$$

Thus, Theorem 1 is correct when $k=1$.

2) when $k=2$, from (27) and Lemma 1, we obtain

$$|\ln\hat{q}_{e_2}| \le |\ln\hat{q}_{e_{1'1}}| + |\ln\hat{q}_{e_{2'2}}| + 2\epsilon|\boldsymbol{p}^b_{d_{12}}|\sin\frac{|\boldsymbol{\theta}_{e_1}|}{2}.$$

Thus, Theorem 1 is correct when $k=2$.

3) when $k=3$, from (28) and Lemma 1, we obtain

$$\begin{aligned}|\ln\hat{q}_{e_3}| &\le |\ln(Ad_{\hat{q}^*_{d_{12}}}\hat{q}_{e_{1'1}} \circ \hat{q}_{e_{2'2}})| + |\ln\hat{q}_{e_{3'3}}| \\ &\quad +2\epsilon|\boldsymbol{p}^b_{d_{23}}|\sin\tfrac{|\boldsymbol{\theta}_{e_2}|}{2} \\ &\le |\ln\hat{q}_{e_{1'1}}| + |\ln\hat{q}_{e_{2'2}}| + |\ln\hat{q}_{e_{3'3}}| \\ &\quad +2\epsilon(|\boldsymbol{p}^b_{d_{12}}|\sin\tfrac{|\boldsymbol{\theta}_{e_1}|}{2} + |\boldsymbol{p}^b_{d_{23}}|\sin\tfrac{|\boldsymbol{\theta}_{e_2}|}{2}).\end{aligned}$$

Thus, Theorem 1 is correct when $k=3$.

4) assume that Theorem 1 holds for $k=N$, i.e.,

$$\begin{aligned}&|\ln\hat{q}_{e_N}| \\ &\le \sum_{i=1}^{N}|\boldsymbol{\theta}_{e_{i'i}}| + \epsilon(\sum_{i=1}^{N}|\boldsymbol{p}^b_{e_{i'i}}| + 2\sum_{j=1}^{N-1}|\boldsymbol{p}^b_{d_{j(j+1)}}|\sin\frac{|\boldsymbol{\theta}_{e_j}|}{2}).\end{aligned} \tag{31}$$

When $k=N+1$, from (25), we obtain

$$\hat{q}_{e_{N+1}} = Ad_{\hat{q}^*_{d_{N(N+1)}}}\hat{q}_{e_N} \circ \hat{q}_{e_{(N+1)'(N+1)}}.$$

According to Lemma 1 and then using (31), it follows:

$$\begin{aligned}&|\ln\hat{q}_{e_{N+1}}| \\ &\le |\ln\hat{q}_{e_N}| + |\ln\hat{q}_{e_{(N+1)(N+1)}}| + 2\epsilon|\boldsymbol{p}^b_{d_{N(N+1)}}|\sin\frac{|\boldsymbol{\theta}_{e_N}|}{2} \\ &\le \sum_{i=1}^{N}|\boldsymbol{\theta}_{e_{i'i}}| + \epsilon(\sum_{i=1}^{N}|\boldsymbol{p}^b_{e_{i'i}}| + 2\sum_{j=1}^{N-1}|\boldsymbol{p}^b_{d_{j(j+1)}}|\sin\frac{|\boldsymbol{\theta}_{e_j}|}{2}) \\ &\quad + |\ln\hat{q}_{e_{(N+1)'(N+1)}}| + 2\epsilon|\boldsymbol{p}^b_{d_{N(N+1)}}|\sin\frac{|\boldsymbol{\theta}_{e_N}|}{2} \\ &= \sum_{i=1}^{N+1}|\boldsymbol{\theta}_{e_{i'i}}| + \epsilon(\sum_{i=1}^{N+1}|\boldsymbol{p}^b_{e_{i'i}}| + 2\sum_{j=1}^{N}|\boldsymbol{p}^b_{d_{j(j+1)}}|\sin\frac{|\boldsymbol{\theta}_{e_j}|}{2}).\end{aligned}$$

Thus, Theorem 1 also holds for $k=N+1$.

Consequently, by induction, the conclusion follows. ■

B. Formation Design

In the sense of error propagation, Theorem 1 provides a safety bound on the formation error. Given a safety specification, i.e., an angular error threshold T_a and a distance error threshold T_d, we are able to estimate the maximal number of rigid-bodies allowed to be embodied in one path for the formation, denoted by $N_{\max}$, such that the overall system's trajectories remain safe at all times. To obtain $N_{\max}$, firstly we find two maximal integers, denoted by N_a and N_d, satisfy the angular and distance error thresholds, respectively. Specifically, in (30), denote $f_\theta(k) = \sum_{i=1}^{k} |\boldsymbol{\theta}_{e_{i'i}}|$ and $f_p(k) = \sum_{i=1}^{k} |\boldsymbol{p}^b_{e_{i'i}}| + 2\sum_{j=1}^{k-1} |\boldsymbol{p}^b_{d_{j(j+1)}}| \sin\frac{|\boldsymbol{\theta}_{e_j}|}{2}$, then N_a and N_d should satisfy the following inequalities:

$$\begin{cases} f_\theta(N_a) \leq T_a < f_\theta(N_a+1), \\ f_p(N_d) \leq T_d < f_p(N_d+1). \end{cases} \tag{32}$$

And then considering the lead, we obtain

$$N_{\max} = \min(N_a, N_d) + 1. \tag{33}$$

Note that $N_{\max}$ obtained from (32)–(33) also can be treated as the maximum depth of the rooted tree. Thus, it provides a rough estimation about the satisfiable number of the rigid-bodies allowed to be embodied in each path or the maximum depth of the rooted tree, with a prior knowledge of errors $|\boldsymbol{\theta}_{e_{i'i}}|$, $|\boldsymbol{p}^b_{e_{i'i}}|$ and $|\boldsymbol{p}^b_{d_{j(j+1)}}|$. In the following, we give an example with a simple scenario to demonstrate its application.

For simplicity, we assume that all $\hat{q}_{d_{i(i+1)}}$s in (25) have the same logarithmic norm in the scenario, i.e., $|\ln \hat{q}_{d_{i(i+1)}}| = \alpha + \epsilon d$ where $\alpha, d > 0$. And further we assume that the angular error and the distance error for every rigid-body are no more than $10\%\alpha$ and $10\%d$, i.e., $|\boldsymbol{\theta}_{e_{i'i}}| \leq 10\%\alpha$ and $|\boldsymbol{p}^b_{e_{i'i}}| \leq 10\%d$. Then given the safety specifications $T_a = \frac{\alpha}{2}$ and $T_d = \frac{d}{2}$, when $\alpha = \frac{\pi}{12}$, we can obtain $N_a = 5$ and $N_d = 3$ by solving (32), so $N_{\max} = 4$. Assuming there exists 15 rigid-bodies in the overall system, one formation structure satisfying the constraints is provided in Fig. 4.

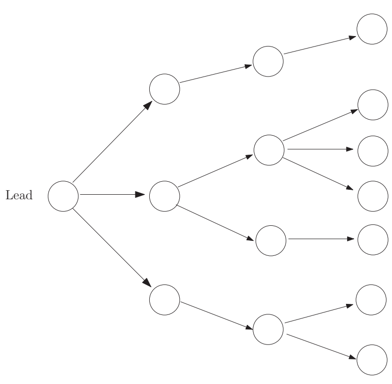

Fig. 4. One example of rooted trees that satisfy the upper bound constraint on depth.

VI. VALIDATION ON USARSIM

We will validate the proposed depth condition for the rooted tree with the scenario in above example. The validations are running on the urban search and rescue simulation (USARSim) platform with a typical UAV, quad-rotor, shown in Fig. 5 (More details about the USARSim platform and the quad-rotor model, refer to http://usarsim.sourceforge.net).

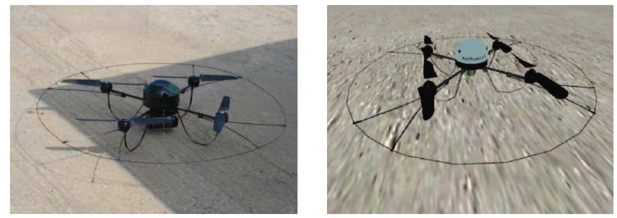

(a) The prototype of quad-rotor (b) Virtual model in USARSim

Fig. 5. The quad-rotor and its virtual model in USARSim

The workspace of quad-rotor is $SO(2)\otimes R^3$, which is with 1 rotational DOF and 3 translational DOF. In $SO(2)\otimes \mathbb{R}^3$, we take z-axis as the rotational axis, and denote angle θ_{zi} relates to $SO(2)$ and position (x^b_i, y^b_i, z^b_i) relates to $\mathbb{R}^3$. Then the configuration of quad-rotor i can be specified by

$$\begin{aligned} \hat{q}_i =& [\cos\frac{\theta_{zi}}{2}, 0, 0, \sin\frac{\theta_{zi}}{2}] \\ &+ \frac{\epsilon}{2}[\cos\frac{\theta_{zi}}{2}, 0, 0, \sin\frac{\theta_{zi}}{2}] \circ [0, x^b_i, y^b_i, z^b_i]. \end{aligned} \tag{34}$$

For simplicity, we use $(\theta_{zi}, x^b_i, y^b_i, z^b_i)$ to represent the configuration of quad-rotor i, and $\hat{q}_i$ can be obtained easily from (34).

Clearly, to validate the structure in Fig. 4, it is only required to verify the errors in one path are satisfied the safety specifications. That is, the angular and the distance errors occurring at the leaf node are no more than the given thresholds T_a and T_d, respectively. Thus, we construct a 4 quad-rotor formation in our simulations, in which quad-rotors are followed one by one in a path. The quad-rotors from the lead to the leaf node are denoted by quad-rotor 0 to 3. The position and orientation information of each quad-rotor, and the control signals are sampled at a time interval of 0.03 s.

In simulations, all the relative configurations from quad-rotor $i+1$ to its neighbor i is $(\frac{\pi}{12}, 2, -2, (-1)^i * 2)$ for $i = 0, 1, 2$, which indicates $\alpha = \frac{\pi}{12}$, $d = 2\sqrt{3}$, $T_a = \frac{\pi}{24}$ and $T_d = \sqrt{3}$. Uniformly distributed noises are added in the formations at the beginning of each echo with $|\boldsymbol{\theta}_{e_{i'i}}| \leq 10\%\alpha$ and $|\boldsymbol{p}^b_{e_{i'i}}| \leq 10\%d$ for $i = 1, 2, 3$. Recording the actual and the desired configurations of quad-rotor 3, we can obtain the angular and distance errors of quad-rotor 3 at each echo. The results of 500 echoes are shown in Fig. 6.

It shows clearly in Fig. 6 that all angular errors and distance errors of quad-rotor 3 are less than the given safety specifications.

VII. CONCLUSIONS

In this paper, by utilizing an alternative mathematical tool – the unit dual quaternion, the error propagation along one path in a rooted tree in 3-D space is analyzed. And a depth conditions for the rooted tree with errors is obtained such that both the specified angular and distance error thresholds

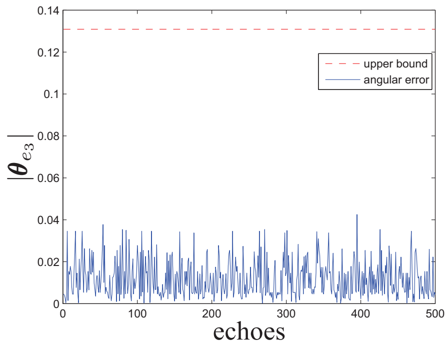

(a) Angular errors and the upper bound

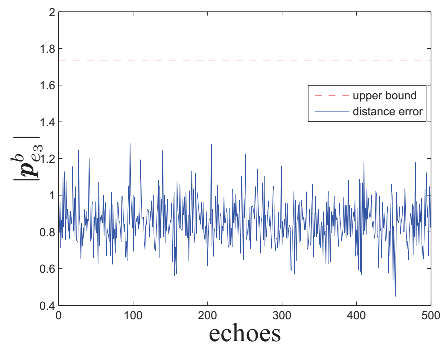

(b) Distance errors and the upper bound

Fig. 6. Angular errors, distance errors and the upper bounds.

can be satisfied, which could be used to guide the design of the formations.

References

[1] N. A. Alsindi, K. Pahlavan, and B. Alavi, "An error propagation aware algorithm for precise cooperative indoor location," in *Proceedings of the IEEE Military Communication Conference*, Washington, DC, USA, 2006, pp. 1–7.

[2] A. I. Mourikis and S. I. Roumeliotis, "Analysis of positioning uncertainty in simultaneous localization and mapping (SLAM)," in *Proceedings of the 2004 IEEE/RSJ International Conference on Intelligent Robots and Systems*, Sendai, Japan, 2004, pp. 13–20.

[3] B. Hu and W. Schiehlen, "Multi-time scale simulation for impact systems: from wave propagation to rigid-body motion," *Archive of Applied Mechanics*, vol. 72, pp. 885–898, 2003.

[4] D. Swaroop and J. K. Hedrick, "String stability of interconnected systems," *IEEE Transactions on Automatic Control*, vol. 41, no. 3, pp. 349–357, 1996.

[5] A. Pant, P. Seiler, and K. Hedrick, "Mesh stability of look-ahead interconnected systems," *IEEE Transactions on Automatic Control*, vol. 47, no. 2, pp. 403–407, 2002.

[6] J. P. Desai, J. P. Ostrowski, and V. Kumar, "Modeling and control of formations of nonholonomic mobile robots," *IEEE Transactions on Robotics and Automation*, vol. 17, no. 6, pp. 905–908, 2001.

[7] J. A. Fax and R. M. Murray, "Information flow and cooperative control of vehicle formations," *IEEE Transactions on Automatic Control*, vol. 49, no. 9, pp. 1465–1476, 2004.

[8] Z. Lin, B. Francis, and M. Maggiore, "Necessary and sufficient graphical conditions for formation control of unicycles," *IEEE Transactions on Automatic Control*, vol. 50, no. 1, pp. 121–127, 2005.

[9] C. Yu, J. M. Hendrickx, B. Fidan, B. D. Anderson, and V. D. Blondel, "Three and higher dimensional autonomous formations: rigidity, persistence and structure persistence," *Automatica*, vol. 43, no. 3, pp. 387–402, 2007.

[10] B. D. Anderson, C. Yu, B. Fidan, and J. M. Hendrickx, "Rigid graph control architecture for autonomous formation," *IEEE Control System Magazine*, vol. 28, no. 6, pp. 48–63, 2008.

[11] J. Funda, R. Taylor, and R. P. Paul, "On homogeneous transformations, quaternions, and computational efficiency," *IEEE Transactionson Robotics and Automation*, vol. 6, no. 3, pp. 382–388, 1990.

[12] J. Funda and R. P. Paul, "A computational analysis of screw transformations in robotics," *IEEE Transactions on Robotics and Automation*, vol. 6, no. 3, pp. 348–356, 1990.

[13] N. Aspragathos and J. Dimitros, "A comparative study of three methods for robot kinematics," *IEEE Transactions on Systems, Man and Cybernetics Part B: Cybernetics*, vol. 28, no. 2, pp. 135–145, 1998.

[14] D. Han, Q. Wei, Z. Li, and W. Sun, "Control of oriented mechanical systems: A method based on dual quaternion," in *17th IFAC World Congress*, Seoul, Korea, 2008, pp. 3836–3841.

[15] X. Wang and C. Yu, "Feedback linearization regulator with coupled attitude and translation dynamics based on unit dual quaternion," in *Proceedings of the 2010 IEEE Multi-Conference on Systems and Control*, Pacifico Yokohoma, Japan, 2010, pp. 2380–2384.

[16] J. S. Goddard, "Pose and Motion Estimation from Vision using Dual Quaternion-based Extended Kalman Filtering," Ph.D thesis, The University of Tennessee, 1997.

[17] K. Daniilidis, "Hand-eye calibration using dual quaternions," *The International Journal of Robotics Research*, vol. 18, no. 3, pp. 286–298, 1999.

[18] Y. X. Wu, X. P. Hu, D. W. Hu, and J. X. Lian, "Strapdown inertial navigation system algorithms based on dual quaternions," *IEEE Transactions on Aerospace and Electronic Systems*, vol. 41, no. 1, pp. 110–132, 2005.

[19] H.-L. Pham, V. Perdereau, B. V. Adorno, and P. Fraisse, "Position and orientation control of robot manipulators using dual quaternion feedback," in *Proceedings of the 2010 IEEE/RSJ International Conference on Intelligent Robots and Systems*, Taipei, Taiwan, 2010, pp. 658–663.

[20] R. M. Murray, Z. Li, and S. S. Sastry, *An Mathematical Introduction to Robotic Manipulation*. CRC Press, 1994.

[21] M.-J. Kim and M.-S. Kim, "A compact differential formula for the first derivative of a unit quaternion curve," *Journal of Visualization and Computer Animation*, vol. 7, no. 1, pp. 43–57, 1996.